

A Novel GaN-on-Si Substrate Power Transistor using Air-Bridge Matrix Structure

Chih-Wei Yang, Hsiang-Chun Wang, Hsien-Chin Chiu

Department of Electronics Engineering, Chang Gung University, Taiwan, R.O.C.

I. Introduction

AlGaIn/GaN high-electron mobility transistors (HEMTs) have potential applications in the next generation of high-power devices. They can maintain robust device characteristics at high temperatures and high voltage conditions because of their superior material properties [56]. Recently GaN on Si (111) technology has found applications in electronic devices because of its low cost and superior scalability of large wafer size [57]. There is an obvious thermal effect observed from the GaN HEMTs on Si substrate due to the current crowding which operated at high voltage condition. The key to solve this problem is to thin the Si substrate. However, this behavior of thin the substrate causes the wafer warp and effects the concentration of 2-DEG. In this study, a novel layout called air-bridge matrix (ABM) device with 100 μm Si substrate was used to reduce the thermal effect. For comparing, the multi-finger (MF) device with different thickness substrate was fabricated at the same process.

II. Device Structure and Fabrication

A 1 μm -thick undoped GaN channel layer was grown on top of a 2 μm -thick undoped AlN/GaN buffer/transition layer and an 18 nm-thick undoped $\text{Al}_{0.27}\text{Ga}_{0.73}\text{N}$ Schottky layer was sandwiched between the GaN channel layer and the 1 nm undoped GaN cap layer. This structure exhibits a sheet charge density of $1.05 \times 10^{13} \text{ cm}^{-2}$ and a Hall mobility of $1483 \text{ cm}^2/\text{V}\cdot\text{s}$ at 300 K. For device fabrication, the active region was protected by a photoresist and the mesa isolation region was removed in a reactive ion etching (RIE) chamber using BCl_3+Cl_2 mixed gas plasma. Ohmic contacts were prepared by the electron beam evaporation of a multilayered Ti/Al/Ni/Au sequence, followed by rapid thermal annealing at 850°C for 30 s in a nitrogen-rich ambient. The ohmic contact resistance is $7.54 \times 10^{-5} \Omega\cdot\text{cm}^2$, as measured by the transmission-line method. In the gate process, a 100-nm-thick Si_3N_4 layer was deposited. As the first passivation layer on the HEMT surface was by PECVD at 280°C . The 3 μm -width T-shaped gate (Ti/Au) was evaporated onto a 2 μm -wide SiN removed gate with a fingers pattern. Finally, the interconnection was deposited as a Ti/Au by using the air-bridge process. Figure 1(a) presents the device structure and cross-section and the device with a $L_{\text{GS}} = 6 \mu\text{m}$, $L_{\text{GD}} = 20 \mu\text{m}$ and $L_{\text{G}} = 2 \mu\text{m}$. Figure 1(b) and 1(c) show the OM image of multi-finger (MF) HEMT and air-bridge matrix (ABM) HEMT, respectively. The active region of both devices is 2.25 mm^2 ($1.5 \text{ mm} \times 1.5 \text{ mm}$) and the Si substrate of both MF and ABM HEMT is thinned to 100 μm .

III. Results and Discussion

Figure 2 displays $I_{\text{DS}}-V_{\text{GS}}$ and $g_{\text{m}}-V_{\text{GS}}$ characteristics of MF and ABM HEMT at $V_{\text{DS}} = 5 \text{ V}$, respectively. An

obvious current improving is observed for MF HEMT due to the air-bridge matrix structure increases the current density from one-dimension to two-dimension. The threshold voltage of both devices is -2.3 V ; and the I_{DS} is 2.1 A of MF HEMT and it can be improved to 4.7 A of ABM HEMT. Figure 3 presents the $I_{\text{DS}}-V_{\text{DS}}$ characteristic of MF HEMT and ABM HEMT with V_{GS} from 1 to -3 V . The $R_{\text{DS, on}}$ was extracted at $V_{\text{GS}} = 0 \text{ V}$; and it is 2Ω for MF HEMT and 0.7Ω for ABM HEMT. The smaller $R_{\text{DS, on}}$ of ABM HEMT is ascribed to the ABM structure improves the current density and reduces the current crowding phenomenon. The current flow of MF HEMT is one-dimension, and the current crowding occurs at the drain electrode due to high electric field. However, the current flow of ABM HEMT is two-dimension, the current can be distributed and current crowding can be weakened. In addition, the DC characteristics of MF HEMT with 1100 μm Si substrate are almost the same with 100 μm Si substrate.

Figure 4 exhibits the off-state breakdown characteristics of MF HEMT with 1100 μm Si substrate, MF HEMT with 100 μm Si substrate, and ABM HEMT with 100 μm Si substrate at $V_{\text{GS}} = -8$. The breakdown measurements were carried out using the Agilent B1505A measurement system. The off-state breakdown voltage (V_{BR}) is defined as the voltage at which a leakage current of 1 mA flows between source and drain electrode. As shown in figure 4, the V_{BR} is 465, 483 and 519 V for MF HEMT with 1100 μm Si substrate, MF HEMT with 100 μm Si substrate, and ABM HEMT, respectively. The ABM HEMT presents a higher V_{BR} .

The thermal images of (a) multi-finger HEMT with 1100 μm Si substrate, (b) multi-finger HEMT with 100 μm Si substrate, and (c) Air-bridge matrix HEMT with 100 μm Si substrate which biases at $V_{\text{DS}} = 5 \text{ V}$, drain current is limited at 1 A, and continuous time is 1 min are shown in Figure 5. The temperature of drain electrode of MF HEMT with 1100 μm Si substrate is 470.1°C and it is fail after the measurement. After thinning the Si substrate to 100 μm , the temperature of drain electrode is reduced to 187.5°C . It is because the heat dispersion of thin substrate is better than thick substrate. However, the temperature can further be reduced to 85.9°C by using ABM HEMT. It can be concluded that the ABM HEMT significantly eliminates the self-heating effect which biases at high voltage.

IV. Conclusion

We have successfully demonstrated the significant enhancement of drain current and eliminated the self-heating effect by using air-bridge matrix HEMT. The I_{DS} of 4.7 A is twice of traditional multi-finger HEMT of 2.1 A. For ABM HEMT, the V_{BR} is improved from 465 to 519 V and the device temperature which biased at $V_{\text{DS}} = 5 \text{ V}$ and $I_{\text{DS}} = 1 \text{ A}$ can be reduced from 470.1 to 85.9°C .

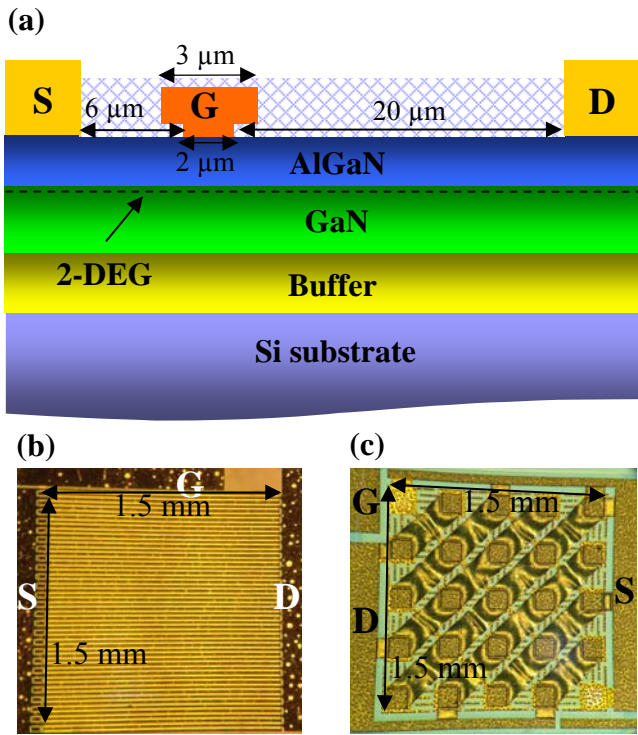


Fig.1(a) Device structure and cross-section of AlGaIn/GaN HEMT with a $L_{GS} = 6 \mu\text{m}$, $L_{GD} = 20 \mu\text{m}$ and $L_G = 2 \mu\text{m}$. (b) Traditional multi-finger device. (c) Air-bridge matrix device.

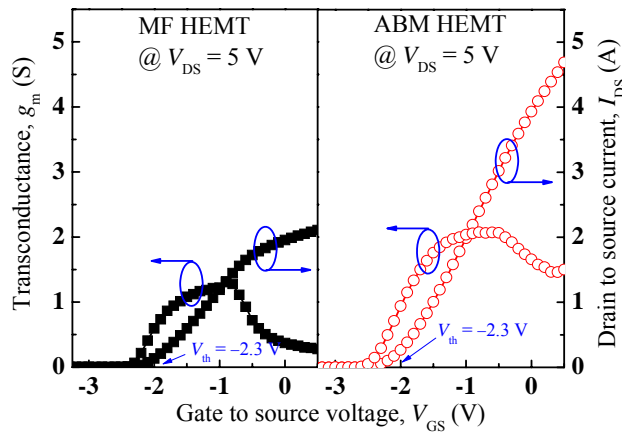


Fig.2 $I_{DS}-V_{GS}$ and g_m-V_{GS} characteristic of multi-finger and air-bridge matrix device at $V_{DS} = 5 \text{ V}$.

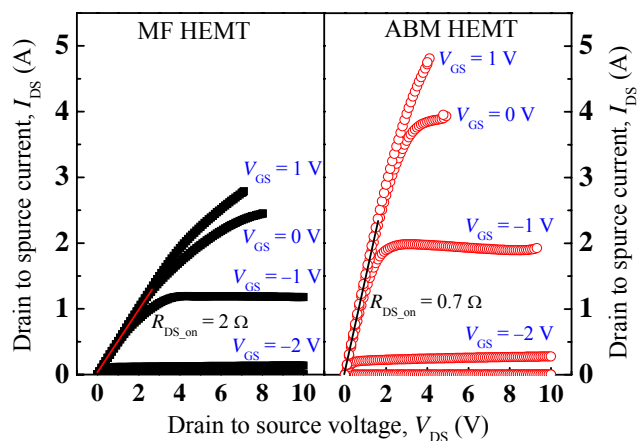


Fig.3 $I_{DS}-V_{DS}$ characteristic of multi-finger and air-bridge matrix device with V_{GS} from 1 to -3 V . $R_{DS(on)}$ was extracted at $V_{GS} = 0 \text{ V}$.

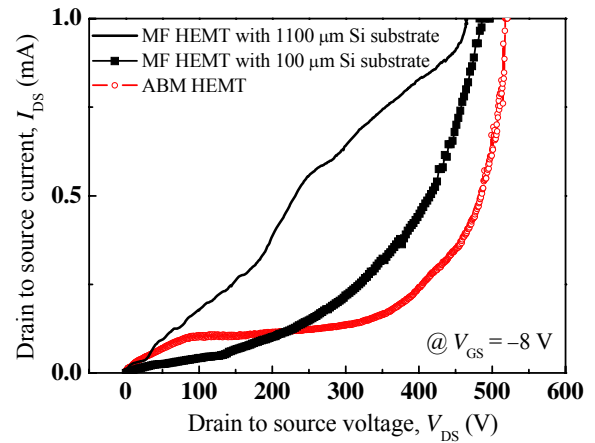


Fig.4 Off-state breakdown voltage of three HEMTs at $V_{GS} = -8 \text{ V}$.

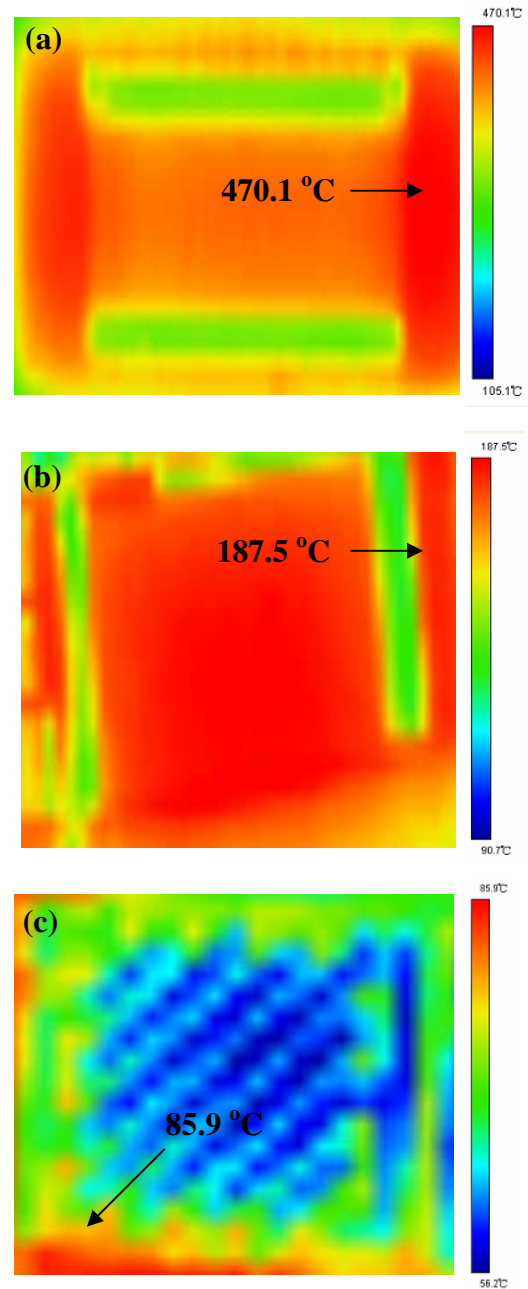


Fig.5 Thermal images of (a) multi-finger HEMT with $1100 \mu\text{m}$ Si substrate, (b) multi-finger HEMT with $100 \mu\text{m}$ Si substrate, and (c) Air-bridge matrix HEMT with $100 \mu\text{m}$ Si substrate which biases at $V_{DS} = 5 \text{ V}$, drain current is limited at 1 A , and continuous time is 1 min .